Available online at www.sciencedirect.com

ScienceDirect

Ceramics International 39 (2013) 9071–9078

CERAMICS INTERNATIONAL

www.elsevier.com/locate/ceramint

The use of egg shells to produce Cathode Ray Tube (CRT) glass foams

Hugo R. Fernandes[a], Fernanda Andreola[b], Luisa Barbieri[b], Isabella Lancellotti[b], Maria J. Pascual[c], José M.F. Ferreira[a,*]

[a]Department of Materials Engineering and Ceramics, University of Aveiro, CICECO, 3810-193 Aveiro, Portugal
[b]Department of Engineering "Enzo Ferrari", University of Modena and Reggio Emilia, via Vignolese 905, I-41125 Modena, Italy
[c]Instituto de Cerámica y Vidrio (CSIC), C/Kelsen 5, Campus de Cantoblanco, 28049 Madrid, Spain

Received 21 March 2013; received in revised form 30 April 2013; accepted 1 May 2013
Available online 9 May 2013

Abstract

Cleaned Cathode Ray Tube (CRT) (panel and funnel) waste glasses produced from dismantling TV and PC colour kinescopes were used to prepare glass foams by a simple and economic processing route, consisting of a direct heating of glass powders at relatively low temperatures (600–800 °C). This study reports on the feasibility of producing glass foams using waste egg shells as an alternative calcium carbonate-based (95 wt%) foaming agent derived from food industry. The foaming process was found to depend on a combination of composition, processing temperature and mixture of raw materials (glass wastes). Hot stage microscopy (HSM), X-ray diffraction (XRD) and scanning electron microscopy (SEM) were used to characterize foams and evaluate the foaming ability and the sintering process. The experimental compositions allowed producing well sintered glass foams with suitable properties for some functional applications with environmental benefits such as: (1) reduced energy consumption because of the low heat treatment temperatures used; and (2) materials produced exclusively from residues.

Keywords: A. Sintering; B. Porosity; D. Glass; Glass foams

1. Introduction

Recycling has emerged as a very important environmental issue nowadays due to the diminishing of natural resources and the increasing amounts of industrial solid wastes generated. Glasses are among the materials which attract great interest in the recycling concept. Systematic community projects for collecting and recycling the waste glasses have already been implemented in many developed countries.

Cathode Ray Tube (CRT) glasses represent about one third of electronics waste tonnage [1]. From the total weight of a computer monitor or a television set about 65% corresponds to CRT which contains hazardous and heavy elements such as lead, cadmium or mercury, for instance [2–4]. The CRT unit is constituted by several glass components divided into three main typologies with different chemical compositions and properties: (1) screen or panel (P, 65%), (2) cone or funnel (F, 30%) and (3) neck (5%). A lead frit is used as seal junction [2]. In fact, cone and neck glasses contain principally lead and other dangerous elements, while panel glass has other heavy metals (Ba, Sr, etc.) which forbid their recycling in the glass industry for the production of containers, domestic glassware and glass fibers.

The collected monitors are usually dismantled and treated in order to dispose of any hazardous materials or components correctly and recycle to the maximum. Processing of a CRT TV or monitor requires specific treatment of the cathode ray tube in order to avoid the release of heavy metal particles and subsequent treatment of the funnel and panel glass. Indeed, in a CRT television set more than 90% of the materials can be recovered for recycling, these include copper (3%), iron (12%), glass (48%) and plastic (17%). As can be seen, the main component is glass that accounts for almost 50% of a TV's overall weight [5].

Until recently, CRT glass closed recycling (which has been estimated up to 30 wt% cone and 10 wt% panel) was an established practice where the glasses were reutilized by the TV manufacturing industry itself with most of the material being sold to Asiatic countries. Nowadays, the event of the new LCD technologies provoked a drastic reduction in the

*Corresponding author. Tel.: +351 234 370242; fax: +351 234 370204.
E-mail address: jmf@ua.pt (J.M.F. Ferreira).

0272-8842/$ - see front matter
http://dx.doi.org/10.1016/j.ceramint.2013.05.002

production of cathode ray tube TVs. This situation evidences the necessity to identify alternative uses for the glass obtained from treatment of TVs and monitors in order to avoid landfill disposal [6]. In this way, some investigations have been developed in diverse fields such as porcelain stoneware production, tableware glass, glass-ceramics, glazes, clay bricks and roof tiles, insulating glass fiber or glass foams [6–12].

One of the most promising and emerging directions for processing of CRT glass is the production of foamed glasses. Glass foam is generally obtained by the action of a gas-generating agent (foaming agent), which is ground together with the starting waste glass to a finely divided powder. The mixture of glass powder, foaming agent, and occasionally other mineral agents is then heat treated at a suitable temperature to promote viscous flow sintering and the thermal decomposition of the foaming agent. The evolution of gas inside the softened pyroplastic mass of glass causes the expansion of the structure. The properties of finished foamed glass products depend strongly on the type and quantity of the added foaming agents, on the initial size of the glass particles, and on the firing schedule [13].

The route here proposed for foaming CRT glasses involves the addition of waste egg shells which act as foaming agent at the processing temperature because it is primarily made up of calcium carbonate ($CaCO_3$) [14,15]. The release of gas (CO_2) inside the softened glass leads to the foam formation. The aim of this work was to investigate the potential of waste egg shells as foaming agent and to evaluate the feasibility of the foaming process and the properties of glass foams produced from CRT glasses. Moreover, the optimization of the foaming process by selecting the best processing parameters including the maximization of the incorporation of glass wastes and the use of low processing temperatures is also desirable.

Table 1
Chemical composition of CRT glass (wt%).

Oxide	Panel (P)	Funnel (F)
SiO_2	67.25	58.84
Al_2O_3	2.76	3.73
Na_2O	7.89	6.60
K_2O	7.56	7.33
CaO	1.34	3.24
MgO	0.36	1.47
BaO	11.31	1.80
SrO	0.26	0.09
PbO	0.13	16.02
Fe_2O_3	0.04	0.12
TiO_2	0.49	0.14
Total	99.39	99.38

2. Experimental procedure

Cullet of panel glass (P) and funnel glass (F) were first crushed in a crushing machine and then dry-milled using a porcelain ball mill. The mean particle size of the glass powders as determined by light scattering technique (Coulter LS 230, CA USA; Fraunhofer optical model) was about 10 μm. Egg shells (E) were milled (~8 μm) and used as foaming agent. Milling the starting waste materials to similar particle sizes will enhance the microstructural homogeneity of the obtained materials [13].

The chemical composition of CRT glass used was determined by XRF spectroscopy (XRF-sequential spectrometer, ARL ADVANT'XP), the data are reported in Table 1.

The thermal characterization of the CRT glass was carried out by DTA analysis (DSC 404, Netzsch) and optical non-contact dilatometer (Misura HSM/ODHT, Expert System Solutions, srl). The data reported in Table 2 show the low-melting nature, related to the glass transition temperature (T_g) determined by DTA analysis. The low softening temperature (T_s), and the high values of the thermal expansion coefficient (α) are in agreement with the relevant quantities of alkaline oxides contained in the glassy network (~15 wt%, Table 1).

Concerning waste egg shells, H-D calcimeter was used to determine the real carbonates content (~95.17 wt%). X-ray analysis was carried out by a powder diffractometer with Ni-filtered Cu Kα radiation (PW 3710, Philips) in the 5–70° 2θ range on the powdered egg shells samples (< 25 μm in size).

Table 3 shows the batch compositions of the investigated glass foams. The mixtures of the powders of P, F and E were dry mixed in a cylindrical rotary mixer for 30 min. Cylindrical pellets (∅ = 20 mm) were prepared by uniaxial pressing (40 MPa). The green samples were heat treated in the temperature range of 600–850 °C in air for 15 min (heating rate $\beta = 5\ K\ min^{-1}$) in order to evaluate the influence of composition (glass waste type and foaming agent content) and processing temperature in the properties of produced glass foams.

The following characterization techniques were employed: (1) the absolute density was measured using a He pycnometer (Micromeritics Accupyc 1330, USA); (2) the apparent density of materials was determined by measuring the weight and the dimensions of the produced materials; (3) the porosity was evaluated according to Eq. (1), where P_0 is porosity (%), d_a is

Table 2
Thermal characterization of CRT glasses.

Type of glass	T_g (°C)[a]	T_s (°C)[b]	α (10^{-6} K^{-1})[b]
Panel (P)	535	720	9.85
Funnel (F)	505	670	9.60

[a]DTA analysis.
[b]Optical dilatometric analysis.

Table 3
Batch compositions of prepared foams (wt%).

Sample	Panel (P)	Funnel (F)	Egg shells (E)
$P_{99}E_1$	99	–	1
$P_{97}E_3$	97	–	3
$P_{95}E_5$	95	–	5
$F_{99}E_1$	–	99	1
$F_{97}E_3$	–	97	3
$F_{95}E_5$	–	95	5

apparent density and d_b is bulk density;

$$P = \left(1 - \frac{d_a}{d_b}\right) \times 100 \quad (1)$$

(4) crystalline phases formed were identified by X-ray diffraction analysis (XRD, Rigaku Geigerflex D/Mac, C Series, Cu Kα radiation, Japan); (5) a side-view hot-stage microscope (HSM, Leitz Wetzlar, Germany) equipped with a Pixera video-camera and image analysis system was used to investigate the sintering behavior of glass powder compacts; (6) the compression strength of cubic samples of about 30 mm edges, placed between parallel plates of stainless steel, was measured in a Shimadzu machine (Trapezium 2, Japan, displacement 0.5 mm min^{-1}); and (7) microstructure observations were done by scanning electron microscopy (SEM, Hitachi SU-70, Japan).

3. Results and discussion

3.1. Glass foaming ability, apparent density and mechanical strength

All compositions showed foaming ability upon heat treatment, although the volume expansions of the samples, the pore dimensions and pore density distributions have varied with the composition and the thermal treatment schedule. Fig. 1a illustrates the values of apparent density obtained for compositions comprising a fixed value of 3 wt% of foaming agent (*i.e.* $P_{97}E_3$ and $F_{97}E_3$) sintered at different temperatures for 15 min (Table 4). The composition comprising funnel glass ($F_{97}E_3$) achieved density values below 0.4 g cm^{-3} at 650 °C (0.35 g cm^{-3}), while the composition containing panel glass ($P_{97}E_3$) needed temperature about 50 °C higher to attain similar apparent density value (0.38 g cm^{-3} at 700 °C). This effect is probably due to the higher refractoriness of glass P that features T_s about 100 °C higher than glass F (Table 2), which prevented the glass attain a viscosity low enough to allow the foaming effect. Increasing the processing temperature above 650 °C resulted in relative small density changes (0.28–0.38 g cm^{-3}) in the foams derived from the $F_{97}E_3$ composition, whilst the foams produced from the $P_{97}E_3$ composition showed larger density variations (0.25–0.64 g cm^{-3}). These results suggest that P glass is more sensitive to temperature variations in the temperature range 650–800 °C than F glass. Considering just a single decimal digit, one might state that the density values of the produced glass foams lie in the range ~0.3–0.4 g cm^{-3} for temperatures higher than 650 °C in the case of $F_{97}E_3$ and higher than 700 °C for $P_{97}E_3$.

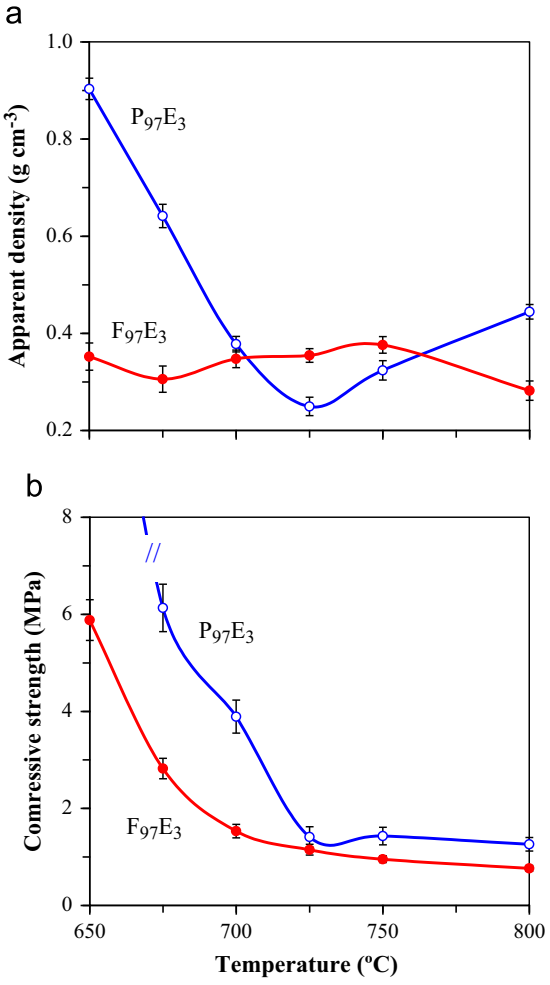

Fig. 1. Evolution of physical properties with sintering temperature for compositions $F_{97}E_3$ and $P_{97}E_3$ of: (a) apparent density and (b) compressive strength.

The results of compressive strength for compositions $P_{97}E_3$ and $F_{97}E_3$ sintered at different temperatures for 15 min are illustrated in Fig. 1b. Generally, these results are in accordance with the variation of apparent density, *i.e.* less dense samples feature lower mechanical resistance. Nevertheless, P-containing compositions present higher mechanical strength than F-containing ones, even when apparent density values are lower than those presented by $F_{97}E_3$ (*e.g.* 725 and 750 °C). This is probably due to the total

porosity of the samples and the microstructure of the struts in the triple points between pores. In fact, for similar values of apparent density, F-containing glass foams feature higher porosity percentage than P-containing ones due to the higher contribution of bulk density of glass F (2.96 g cm^{-3}) in comparison to glass P (2.74 g cm^{-3}), which is mainly caused by the presence of PbO in glass F (Table 1, Eq. (1)) can explain the compressive strength tendency observed for these compositions.

The effect of the foaming agent content on glass foaming ability was evaluated via sintering of samples at 700 °C for 15 min with varying E content in the range 0–5 wt%. The results are expressed as evolution of apparent density with the temperature as shown in Fig. 2. Both groups of compositions, *i.e.* those derived from panel glass ($P_{100-x}E_x$) and from funnel glass ($F_{100-x}E_x$), feature the same trend: (1) small incorporation of E (1 wt%) result in relatively high values for apparent density (1.1 and 0.6 g cm^{-3} for $P_{100-x}E_x$ and $F_{100-x}E_x$, respectively); (2) the increase of E to 2 wt% resulted in a strong decrease of the apparent density (more evidenced for $P_{100-x}E_x$), and (3) further increasing of E ($x=3-5$) led to a stabilization of the density values in the range 0.3–0.4 g cm^{-3}. These results suggest that the optimum content of E in order to obtain high porous samples should be near 3 wt% under the experimental conditions.

Table 4
Apparent density and compressive strength values of glass foams sintered for 15 min at several temperatures.

T (°C)	Density (g cm^{-3})		Compressive strength (MPa)	
	$F_{97}E_3$	$P_{97}E_3$	$F_{97}E_3$	$P_{97}E_3$
650	0.56 ± 0.03	0.90 ± 0.02	5.88 ± 0.42	14.82 ± 0.68
675	0.41 ± 0.03	0.64 ± 0.02	2.82 ± 0.21	6.13 ± ±0.49
700	0.35 ± 0.02	0.38 ± 0.01	1.53 ± 0.14	3.89 ± 0.34
725	0.35 ± 0.01	0.29 ± 0.02	1.15 ± 0.11	1.41 ± 0.21
750	0.38 ± 0.01	0.32 ± 0.02	0.95 ± 0.07	1.43 ± 0.18
800	0.28 ± 0.02	0.44 ± 0.01	0.76 ± 0.06	1.26 ± 0.14

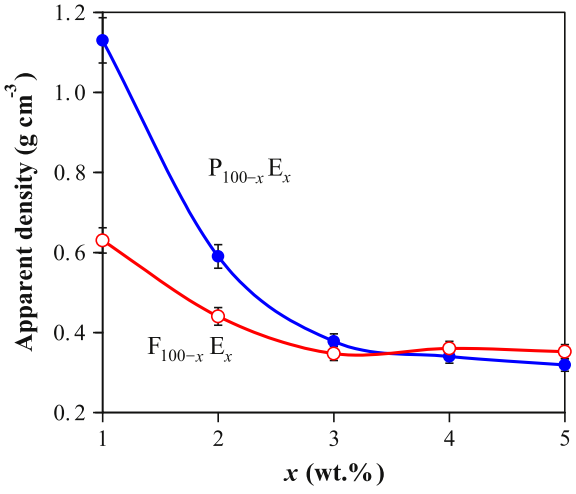

Fig. 2. Evolution of apparent density with the content of foaming agent E for compositions sintered at 700 °C for 15 min.

3.2. Analysis of the foaming mechanism by HSM

There are several important characteristic viscosity points based on the relation between the temperatures measured by HSM and corresponding viscosities (Table 5) [16,17]. A/A_0 corresponds to the ratio of final area/initial area of the glass-powder compacts. T_D is an important and determinant temperature in the foaming process since glass attains enough low viscosity which allows the sample to expand under the pressure produced by gas releasing from the decomposition process of the foaming agent. However, if the viscosity is too low the structure can collapse due to gravity effect and a high porous sample could not be obtained.

An optimum thermal treatment is when the foaming agent evolves gas while the glassy phase has a viscosity between 10^7–10^8 poise, which permits producing a homogeneous porosity. In order to support these results, a theoretical calculation by software of Lakatos viscosity as a function of the temperature has been performed for the two CRT glass compositions [18]. The method is based on the linear dependence between the glass constituent concentrations expressed in mol% and the viscosity (standard deviation ~3.01 °C). The interactions among the glass constituents have not been considered. From the theoretical calculations, it has been possible to estimate the viscosity of the P and F glasses in the range $\log \eta = 2$ to $\log \eta = 13.4$. At $\log \eta = 7.6$, the corresponding temperatures for the P and F glass were 709 and 693 °C, respectively.

Table 5
Important characteristic viscosity points based on the relation between the temperatures measured by hot stage microscopy and corresponding viscosities.

		$\log \eta$ (dPa s)	Description
T_{FS}	First shrinkage	9.1 ± 0.1	Temperature at which the pressed sample starts to shrink
T_{MS}	Maximum shrinkage	7.8 ± 0.1	Temperature at which maximum shrinkage of the glass-powder compact is achieved before it starts to soften
T_D	Softening point	6.3 ± 0.1	Temperature at which the first signs of softening are observed (generally shown by the disappearance or rounding of the small protrusions at the edges of the sample)
T_{HB}	Half ball point	4.1 ± 0.1	Temperature at which the section of the observed sample forms a semicircle on the microscope grid
T_F	Flow point	3.4 ± 0.1	Temperature at which the maximum height of the drop of the molten glass corresponds to a unit on the microscopic scale

The variation in the relative area (A/A_0) with respect to temperature is shown in Fig. 3 while photomicrographs demonstrating a change in the geometrical shape with temperature, as obtained from HSM, are presented in Fig. 4. The estimated value for the beginning of the shrinkage process for composition $P_{99}E_1$ was about 590 °C (Fig. 3a) and shrinkage proceeded with increasing temperature until it reached its maximum at about 668 °C. Increasing the E content to 3 and 5 wt% (Fig. 3b and 3c, respectively) resulted in similar HSM curves and the beginning of the shrinkage process shows slight shift to higher temperatures. Only the composition containing the higher amount of foaming agent ($P_{95}E_5$) shows a slight expansion after the maximum shrinkage was achieved. The composition derived from glass F with 1 wt% E ($F_{99}E_1$) started the shrinkage at lower temperature (559 °C, Fig. 3d) and reached the maximum shrinkage at about 637 °C. Increasing of the foaming agent content in composition $F_{99}E_1$ (Fig. 3e and 3f) did not reflect significant changes in the temperature of first shrinkage, but shifted the temperature of maximum shrinkage to lower values. Moreover, the expansion phenomena is more intense for compositions containing higher E amount as evidenced by the slope of the curves observed in Fig. 3e and 3f. The results evidenced that compositions derived from glass F start the shrinkage process and reach the point of maximum shrinkage at lower temperatures than those derived from glass P. Moreover, $P_{99}E_1$ shows higher maximum shrinkage value than composition $F_{99}E_1$. On the other hand, after the point of maximum shrinkage was attained, the composition $F_{97}E_3$ showed a strong expansion, an effect not observed for composition $P_{99}E_1$. These results are in accordance with the

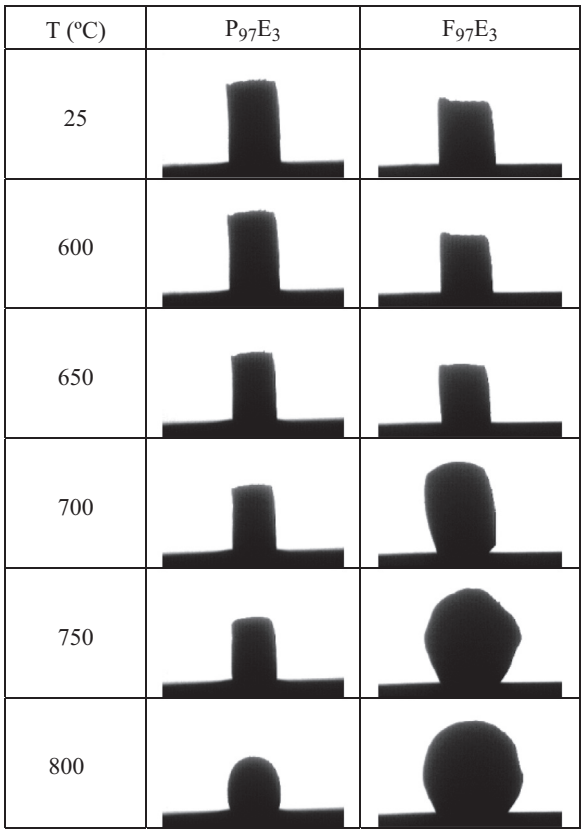

Fig. 4. Hot stage microscopy images of samples with compositions $P_{97}E_3$ and $F_{97}E_3$ on dense alumina substrates.

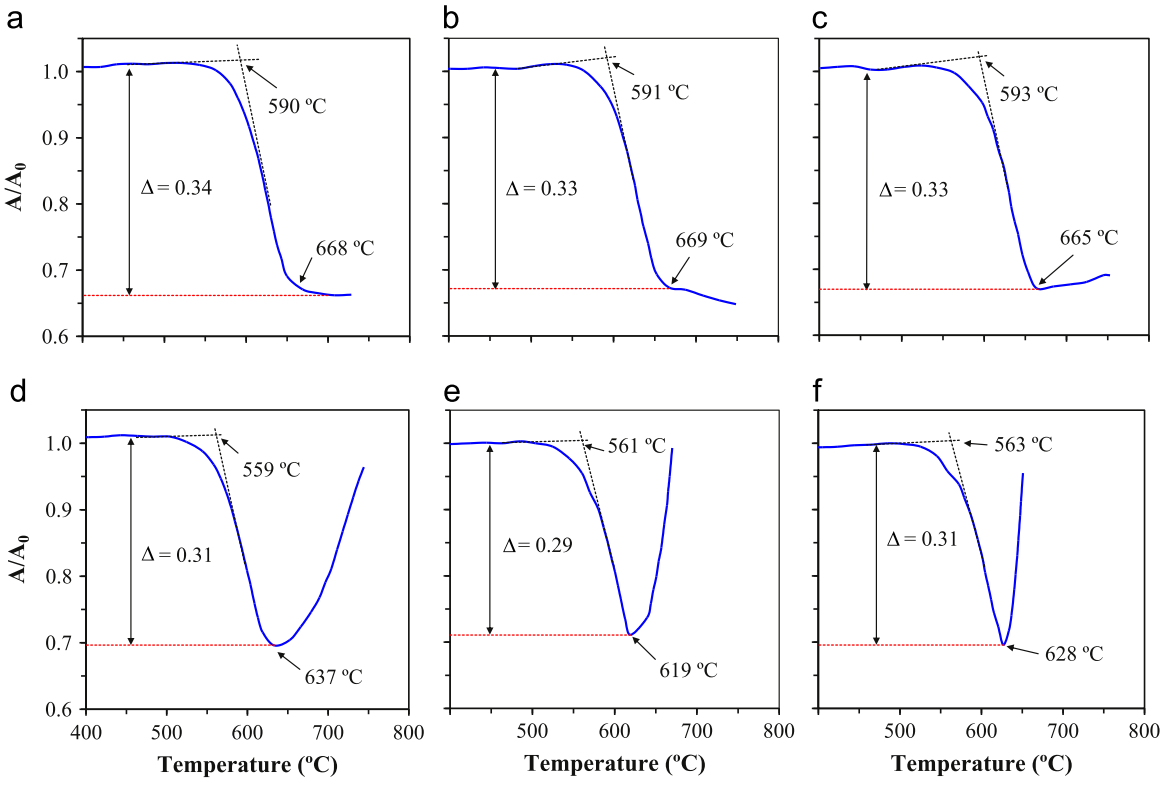

Fig. 3. Variation in the relative area of the glass-powder compacts (A/A_0) *versus* temperature from hot stage microscopy measurements: (a) $P_{99}E_1$, (b) $P_{97}E_3$, (c) $P_{95}E_5$, (d) $F_{99}E_1$, (e) $F_{97}E_3$, and (f) $F_{95}E_5$.

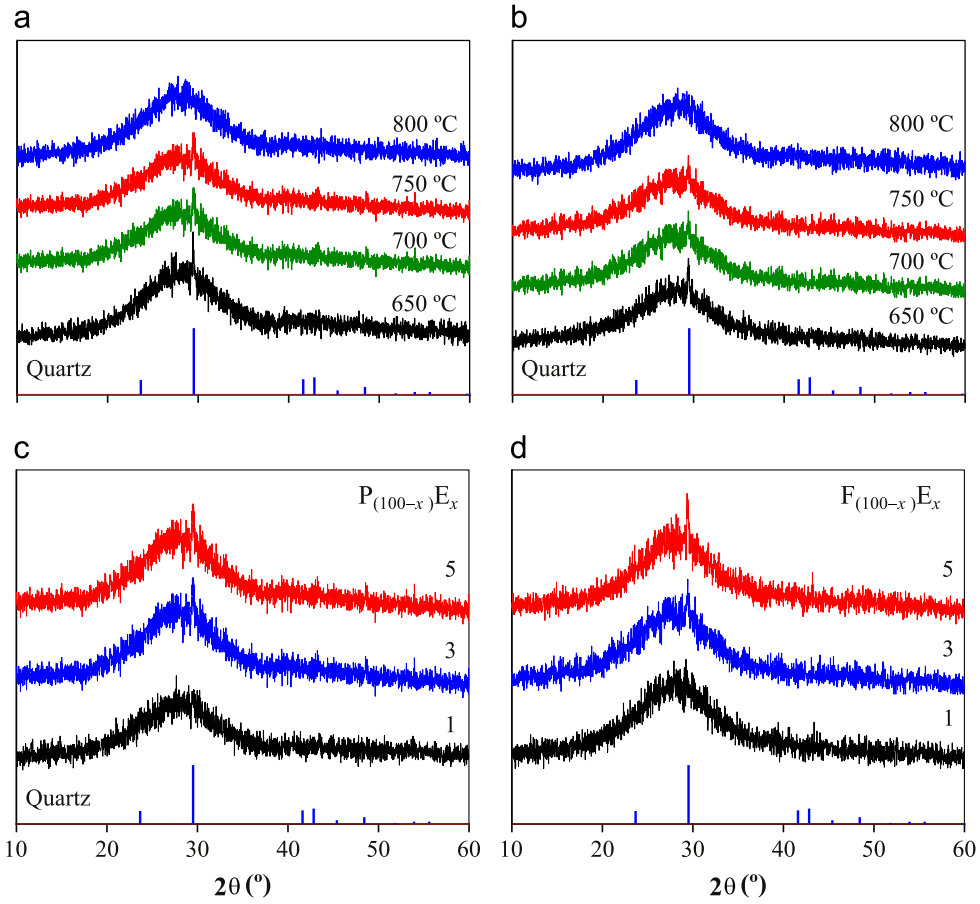

Fig. 5. X-ray diffractograms of glass foams $P_{97}E_3$ (a) and $F_{97}E_3$ (b) sintered at different temperatures for 15 min and compositions $P_{100-x}E_x$ (c) and $F_{100-x}E_x$ (d) containing different amounts of E sintered at 700 °C, with $x=1-5$ wt%.

lower apparent density values presented by composition $F_{97}E_3$ in comparison to $P_{97}E_3$.

No evidence of deformation was observed in samples heat-treated at 600 °C as shown in Fig. 4. At 650 °C, P-containing compositions maintained their original shape while F-containing compositions started evidencing some rounded edges (beginning of deformation). At 700 °C, $F_{97}E_3$ featured the maximum expansion whilst $P_{97}E_3$ kepts its original shape up to 750 °C. At this temperature, $P_{97}E_3$ showed the first signs of deformation and $F_{97}E_3$ reached the beginning of collapse under their own weight due to the attained low viscosity.

These results suggest that composition (*i.e.* the type of glass used in the batch and the foaming agent content) plays an important role in the foaming mechanism. Moreover, they are the evidence that 700 °C is the optimum sintering temperature for F-containing compositions while higher temperatures are required to sinter P-containing compositions.

3.3. Phase assemblage and microstructure of glass foams

The formation of crystalline phases and the extent of crystallization, as well as its dependence of starting composition and sintering temperature, are important factors that determine the structural evolution and the final properties of glass foams. Glass samples sintered at different heat treatments in the temperature range 650–850 °C revealed low crystalline nature as evidenced by the broad X-ray diffractograms presented in Fig. 5. All compositions featured absence of crystalline phases or just a small peak of quartz (ICDD card 070-2538) when sintered at different temperatures or different amounts of foaming agent, evidencing low crystallization ability of the experimental compositions. Moreover, phase assemblage after sintering attains small variations with sintering temperature and composition under the experimental conditions. These results along with the HSM observations (Fig. 3) suggested that these compositions present good sintering behavior.

The type of porous structure, in particular the cells' sizes and thickness of cell walls, plays an important role in the resulting glass foam properties [19]. Fig. 6 illustrates the evolution of microstructure of some experimental glass foams. The effect of temperature on the microstructure of glass foam with P-containing compositions is well evidenced by Figs. 6a–c. At 600 °C the microstructure of $P_{97}E_3$ is characterized by small and homogeneous dispersed pores (Fig. 6a). Increasing the temperature to 700 °C led to increase of pore size maintaining the homogenous appearance (Fig. 6b). Additional temperature increasing (750 °C) resulted in the coarsening of some pores, probably due to coalescence of smaller ones, and the pore size distribution became assorted (not shown). The effect of foaming agent content on the microstructure of P-containing glass foams can be observed in Fig. 6c which correspond to P-containing compositions sintered at

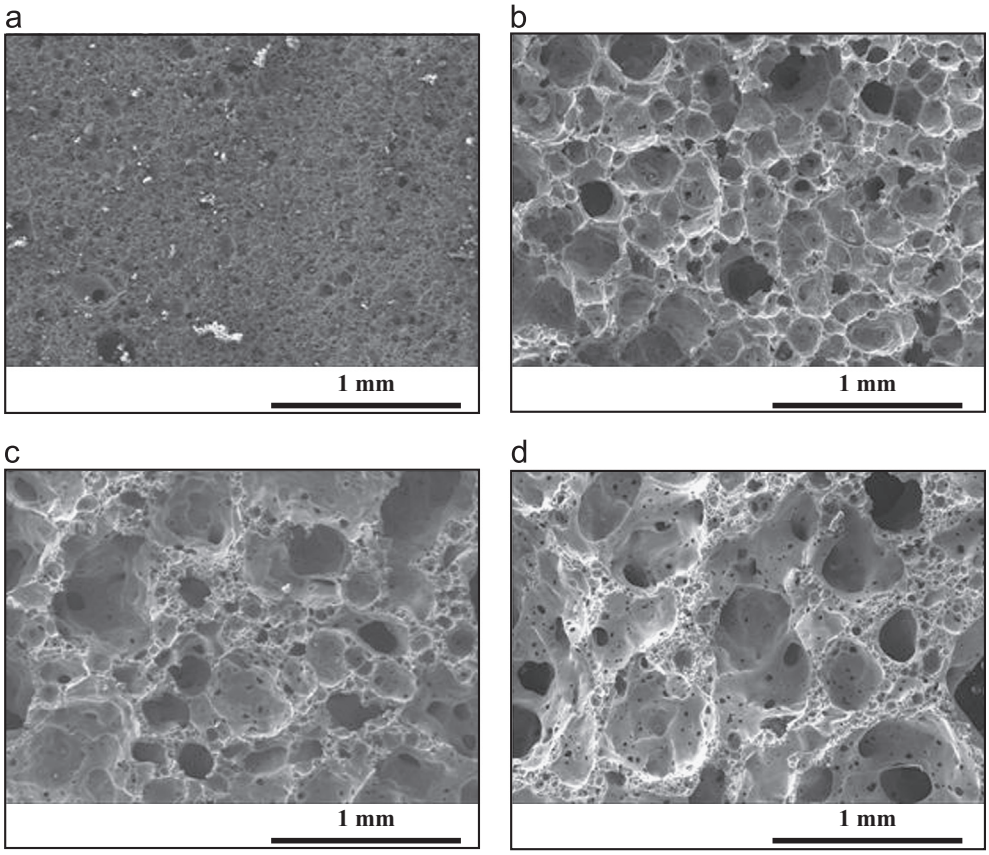

Fig. 6. Microstructures of glass foams: (a) $P_{97}E_3$—600 °C, (b) $P_{97}E_3$—700 °C, (c) $P_{95}E_5$—700 °C and (d) $F_{97}E_3$—700 °C.

700 °C with added 5 wt% of egg shells ($P_{95}E_5$). Higher E content resulted in more intense foaming effect and, consequently, higher pores' sizes. When glass P was replaced by glass F in composition $P_{97}E_3$, the pore sizes increased significantly (Fig. 6d) due to the lower value of softening point of glass F in comparison to that of glass P, which enhanced the foaming effect.

4. Conclusions

The possibility of producing glass foams by using recycling CRT waste glasses (panel and funnel glass) along with egg shells as foaming agent has been presented. Both types of glasses (F and P) with added egg shells as foaming agent revealed to be suitable precursor mixtures for the production of low density ($\sim 0.35\ g\ cm^{-3}$) glass foams. The expansion ability of the precursor mixtures and the developed microstructure in the resulting foams and their physical properties depend on glass composition, the amount of foaming agent added, and the temperature of heat treatment. HSM revealed to be an interesting tool to assess the effects of the experimental variables on the foaming ability.

Egg shells proved to be a good alternative to conventional foaming agents such as $CaCO_3$, $MgCO_3$, or SiC used in the production of glass foams, offering interesting advantages: (i) being a waste material it is potentially cost-free; (ii) its incorporation in glass foams contributes to clean the environment; and (iii) the gas releasing ability at relative low temperatures (700 °C) enables saving energy.

Acknowledgment

Hugo R. Fernandes is grateful for the financial support of CICECO and for the Post Doctoral Grant (SFRH/BPD/86275/2012) from the Fundação para a Ciência e a Tecnologia (FCT), Portugal.

References

[1] F. Mear, P. Yot, M. Cambon, M. Ribes, The characterization of waste cathode-ray tube glass, Waste Management 26 (2006) 1468–1476.
[2] F. Andreola, L. Barbieri, A. Corradi, I. Lancellotti, R. Falcone, S. Hreglich, Glass-ceramics obtained by the recycling of end of life cathode ray tubes glasses, Waste Management 25 (2005) 183–189.
[3] N. Menad, Cathode ray tube recycling, Resources Conservation and Recycling 26 (1999) 143–154.
[4] V. Palm, Swedish Environmental hazards connected to the composition of cathode-ray tubes and cabinets, Environmental Research Institute, Stockholm, 1995.
[5] Glass Plus Project, 2010–2012, 2012.
[6] F. Andreola, L. Barbieri, A. Corradi, I. Lancellotti, CRT glass state of the art—a case study: recycling in ceramic glazes, Journal of the European Ceramic Society 27 (2007) 1623–1629.
[7] F. Andreola, L. Barbieri, E. Karamanova, I. Lancellotti, M. Pelino, Recycling of CRT panel glass as fluxing agent in the porcelain stoneware tile production, Ceramics International 34 (2008) 1289–1295.

[8] E. Bernardo, G. Scarinci, P. Bertuzzi, P. Ercole, L. Ramon, Recycling of waste glasses into partially crystallized glass foams, Journal of Porous Materials 17 (2010) 359–365.
[9] M. Dondi, G. Guarini, M. Raimondo, C. Zanelli, Recycling PC and TV waste glass in clay bricks and roof tiles, Waste Management 29 (2009) 1945–1951.
[10] H.R. Fernandes, D.U. Tulyaganov, J.M.F. Ferreira, Production and characterisation of glass ceramic foams from recycled raw materials, Advances in Applied Ceramics 108 (2009) 9–13.
[11] S. Hreglich, R. Falcone, M. Vallotto, The recycling of EOL panel glass from TV sets in glass fibres and ceramic productions, International Symposium on Recycling and Reuse of Glass Cullet, University of Dundee, Scotland123–134.
[12] D.U. Tulyaganov, H.R. Fernandes, S. Agathopoulos, J.M.F. Ferreira, Preparation and characterization of high compressive strength foams from sheet glass, Journal of Porous Materials 13 (2006) 133–139.
[13] M. Scheffler, P. Colombo, Cellular Ceramics: Structure, Manufacturing, Properties and Applications, Wiley-VCH Verlag GmbH & Co., Weinheim, 2005.
[14] S.V.R. Rao, Plant meal improves eggshells quality, Feed Mix 11 (2003) 28–29.
[15] T.G. Taylor, How an eggshell is made, Scientific American 222 (1970) 88–95.
[16] M.J. Pascual, A. Duran, M.O. Prado, A new method for determining fixed viscosity points of glasses, Physics and Chemistry of Glasses 46 (2005) 512–520.
[17] H. Scholze, Influence of viscosity and surface tension on Hot Stage Microscopy measurements on glasses, Berichte der Deutschen Keramischen Gesellschaft 391 (1962) 63–68.
[18] T. Lakatos, L.G. Johansson, B. Simmingskold, Viscosity–temperature relations in the glass system SiO_2–Al_2O_3–Na_2O–K_2O–CaO–MgO in the composition range of technical glasses, Glass Technology 13 (1792) 88–95.
[19] E. Bernardo, F. Albertini, Glass foams from dismantled cathode ray tubes, Ceramics International 32 (2006) 603–608.